
This is the **accepted version** of the journal article:

Del Corro, Elena; Taravillo, Mercedes; García Baonza, Valentín. «Nonlinear strain effects in double-resonance Raman bands of graphite, graphene, and related materials». *Physical review B : Condensed matter and materials physics*, Vol. 85, Issue 3 (January 2012), art. 033407. DOI 10.1103/PhysRevB.85.033407

This version is available at <https://ddd.uab.cat/record/306920>

under the terms of the  IN COPYRIGHT license

1 Nonlinear strain effects in double-resonance Raman bands of graphite, 2 graphene, and related materials

3 Elena del Corro,^{*} Mercedes Taravillo, and Valentín G. Baonza

4 *MALTA Consolider Team, Departamento de Química Física I, Facultad de Ciencias Químicas, Universidad Complutense de Madrid,
 5 E-28040 Madrid, Spain*

6 (Received 23 November 2011; revised manuscript received 29 December 2011; published xxxx)

7 We analyze the influence of biaxial strain on the double-resonance (*D* and *2D*) Raman bands of graphite-related
 8 materials. A substantial nonlinear dependence of these bands with the strain is observed, evidencing a quite
 9 different effect on the electronic structure around the \mathbf{K} and Γ points of the first Brillouin zone. The strain
 10 dependence of the Grüneisen parameters is also analyzed and discussed. We suggest an application of Raman
 11 spectroscopy in graphite-related systems, based on the frequency difference observed between the *G* and *D* bands
 12 (or half the frequency of the *2D* features in undefective samples), to provide a measure of the local strain.

13 DOI: 10.1103/PhysRevB.00.003400

14 PACS number(s): 63.22.Rc, 07.10.Pz, 81.05.uf, 81.40.Vw

15 The mechanical properties of carbon materials are being
 16 extensively analyzed since the discovery of the exceptional
 17 Young moduli of carbon nanotubes^{1,2} and graphene.³ An
 18 interesting finding is that despite its large intrinsic strength,
 19 graphene exhibits nonlinear elastic behavior under large
 20 deformations, as revealed in atomic-force-microscope nanoin-
 21 dentation experiments³ and combined elasticity theory and
 22 tight-binding atomistic simulations.⁴ Here we demonstrate
 23 that the nonlinear behavior is already noticeable in graphite
 24 under compressive biaxial strains as low as 0.2%, as revealed
 25 by Raman spectroscopy measurements. The purpose of this
 26 letter is to analyze the influence of this behavior on the
 27 double-resonance *D* and *2D* Raman bands^{5–8} of graphite,
 28 graphene, and other related materials.

29 Raman spectroscopy is considered among the most suitable
 30 techniques to characterize the strain response of carbon
 31 materials.⁹ Experiments in graphene under both compressive
 32 and tensile strain along both uniaxial¹⁰ and biaxial directions¹¹
 33 and under hydrostatic conditions^{12,13} are feasible. A common
 34 goal in previous studies was deriving a relation between
 35 the frequency shift of a given Raman band and the applied
 36 strain or, equivalently, defining universally valid Grüneisen
 37 parameters.^{10–12} However, different strain slopes for each
 38 Raman signature have been reported due to factors such as
 39 different stress conditions, the way this stress is transferred to
 40 the sample, and the material in which graphene is supported or
 41 surrounded.^{10–12,14–17} Thus, special care must be taken when
 42 using the Raman spectrum as a strain probe.

43 Recent compressive uniaxial experiments on graphene per-
 44 formed by bending graphene flakes on a plastic substrate^{16,17}
 45 reveal that samples tend to buckle or collapse at relatively
 46 low strains, leading to unavoidable curvature effects and
 47 consequently to a softening of the Raman frequencies at
 48 large compressions. These unwanted effects preclude giving
 49 a definitive conclusion on the nonlinear behavior of graphene
 50 under compressive strain. Theoretical calculations by Mohr
 51 *et al.*¹⁸ also predicted a nonlinear strain dependence for the *D*
 52 band, but experiments of Ding *et al.*¹¹ failed to give a definitive
 53 experimental confirmation of this effect, since they only
 54 reached tensile and compressive biaxial strains around 0.15
 55 and –0.08%, respectively, by utilizing piezoelectric actuators.
 56 It appears that such biaxial strains were too small to confirm

57 the intriguing results of Refs. 16 and 17 and the predictions
 58 of Mohr *et al.*¹⁸ In any case, from the experimental point of
 59 view, the experiments of Ding *et al.*¹¹ confirm the difficulties
 60 that exist in attaining large compressive strains in graphene
 61 with current techniques.

62 The obvious solution for subjecting graphene samples to
 63 large compressions is to perform hydrostatic experiments in
 64 diamond anvil cells (DACs). Raman experiments have been
 65 successfully carried out in both supported and unsupported
 66 samples.^{12,13} The study of Proctor *et al.*¹² confirmed that
 67 unsupported graphene samples behave intrinsically similar to
 68 graphite under compression. Interestingly, a similar conclusion
 69 can also be derived from the work of Nicolle *et al.*¹³ because,
 70 when pressure-induced doping from the surrounding medium
 71 is subtracted, the strain slope for the *G* band of mono- and
 72 bilayer graphene is close to their results in bulk graphite
 73 under pure biaxial compression. This suggests that the pure
 74 mechanical response of graphene and graphite are essentially
 75 the same and, in the absence of additional perturbations,
 76 that the measured vibrational frequencies provide a correct
 77 estimation of the strain. In any case, despite the relevance
 78 of the DAC results, the use of diamond anvils prevents the
 79 observation of the *D* band at moderate strains because of the
 80 coincidence with the intense Raman signature of diamond.¹³
 81 Another possible interference in standard DAC experiments
 82 concerns the interaction of the sample with the surrounding
 83 hydrostatic media, which will be discussed later.

84 Some of the intrinsic experimental drawbacks described
 85 above can be solved with the experimental setup used in this
 86 work. Instead of diamond, the use of moissanite (6H-SiC)¹⁹ or
 87 sapphire²⁰ allows the construction of anvil-based setups that
 88 are more suitable to study the Raman scattering of carbon
 89 materials under biaxial strain or hydrostatic pressure.^{21,22}
 90 In the present experiments, biaxial strain is achieved by
 91 direct compression of the sample between the two moissanite
 92 anvils, as is shown in Fig. 1(a). As discussed in Ref. 11,
 93 uniaxial strain has a significant influence in the electronic
 94 structure of graphene, so biaxial experiments are more suited
 95 to determine pure strain effects, particularly if we want to
 96 analyze the behavior of the double-resonance bands. Another
 97 appealing advantage of our setup is that plastic deformation is
 98 induced in the sample, so residual tensile strain is generated in

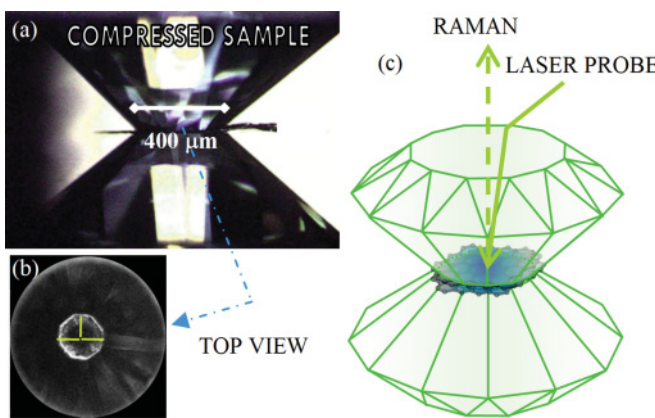


FIG. 1. (Color online) (a) Lateral view of the compressed sample onto the two anvils of a moissanite anvil cell. (b) Frontal view through the top anvil of a compressed sample. The green/light gray lines indicate that the paths along the Raman spectra were recorded. (c) Schematic representation of a compressed graphite sample in a moissanite anvil cell.

some regions with decompression (recovered samples). This allows us to simultaneously study the strain response of the sample under both compressive and tensile regimes in a single experiment. In addition, in this kind of experiment, no pressure media is required, so additional interferences are avoided.

The anvil cell is optically coupled to a micro-Raman spectrometer, which is described elsewhere.²⁰ A Spectra-Physics solid-state laser operating at 532.0 nm was used for the excitation. The typical sampling area was about 1–2 μm in diameter. The spectra were measured at 2 cm⁻¹ spectral resolution and calibrated with a neon emission lamp. The cell is mounted on a XYZ stage, which has an accuracy of 1 μm. Highly oriented pyrolytic graphite (HOPG) discs (3 mm diameter, 60 μm thickness) were purchased from SPI Supplies, from which our samples were prepared. An example of one of our samples is given in Fig. 1(b), where the darker region centered on the sample corresponds to the area subjected to larger biaxial stresses. We recorded the Raman spectra at different distances from the center of the compressed sample following the radial paths indicated in Fig. 1(b). The compression was subsequently released, the cell opened, and the recovered sample characterized along the same paths. Several runs were performed at different values of the maximum stress in order to check the reproducibility of our measurements and to confirm that the observed behavior does not depend on the maximum stress generated on the sample. As expected, we observe upshifts on all of the Raman bands under biaxial strain. Some regions of the sample were recovered under tensile biaxial strain, as confirmed by the downshifts in the frequencies of the D , G , and $2D$ bands, thereby corroborating the nonlinear mechanical behavior of the specimens. Examples of the measured spectra under both compressive and tensile strain are compared in Figs. 2(a) and 2(b) with the Raman spectrum of pristine HOPG. In Figs. 2(c) and 2(d), we plot the Raman shifts of the G , D , and $2D$ bands as functions of biaxial strain. The strain was calculated from the shift of the G band, which typically shows an almost linear dependence with the strain.²³ However, the nonlinear dependence of the D band with the strain is evident.

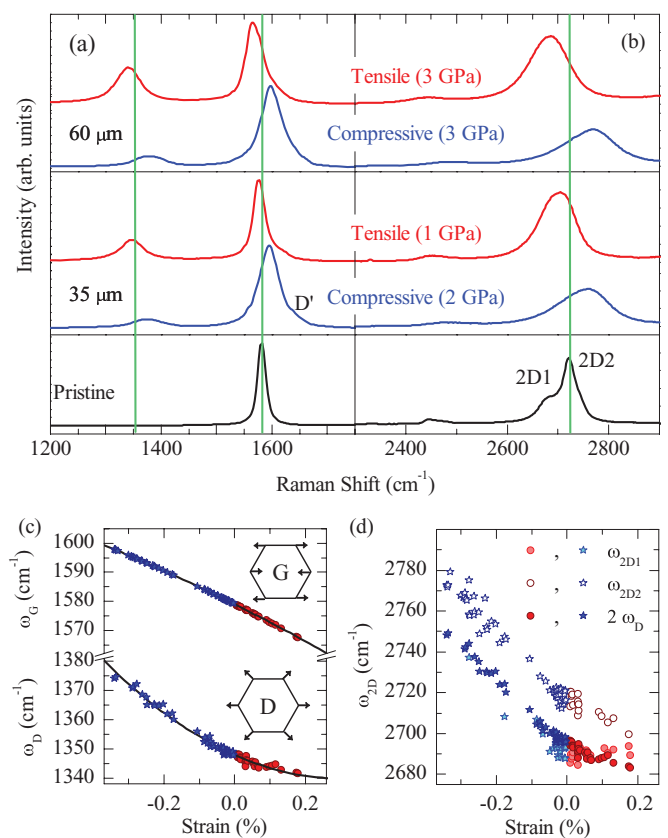


FIG. 2. (Color online) (a), (b) Raman spectra of pristine (black), compressed (blue/dark gray), and recovered (red/gray) graphite samples, in two different radial positions of one of the samples. Numbers (in μm) indicate the distance from the center of the compressed sample. Green/light gray lines indicate the position of the D , G , and $2D2$ bands at ambient conditions and 532 nm excitation (1352, 1582, and 2722 cm⁻¹, respectively). The Raman spectra of the compressed samples have been corrected by the moissanite background, as explained in Ref. 22. Intensities in (b) have been multiplied by a factor of 2. (c) Raman shift of the G and D bands as a function of the biaxial strain applied in a thin graphitic sample. The inserted diagrams represent the atomic displacement movements related to both the D and G bands. (d) Raman shift of the $2D$ contributions ($2D1$ and $2D2$), compared with twice the frequency of the D band, as a function of the biaxial strain. The blue/dark gray stars correspond to the compressed sample and the red/gray circles correspond to the expanded one. In (c), the lines represent the polynomial fitting functions to our results.

Shifts in the in-plane vibrations, like those associated to the D and G bands, as shown in Fig. 2(c), are almost negligible when stress is applied along the c axis. This has been confirmed for the G band in previous studies of graphite under hydrostatic²³ and biaxial stress²⁴ conditions, and this conclusion may be extended to few-layer graphene in view of the results of Nicolle *et al.*¹³ Thus, the stress-induced frequency shift of the G band can be used as a reliable estimate of the local biaxial strain in our measurements. A blue shift of the G band reveals a strengthening of the C-C bond or, in other words, a reduction of the local C-C distance. The pressure dependence of the lattice parameters of graphite has

BRIEF REPORTS

PHYSICAL REVIEW B 00, 003400 (2012)

been previously studied by x-ray diffraction, together with Raman measurements,²³ so a quantitative measure of the strain can be obtained from the relative frequency shift of the *G* band. In the examples shown in Fig. 2, the frequencies measured at 35 and 60 μm from the center of the sample appear around 15 and 10 cm^{-1} , respectively, above the frequency measured at room conditions, which corresponds to compressive strains around -0.32 and -0.23% , respectively. Lower *G*-band frequencies than those measured at room conditions imply that the samples recovered after a biaxial stress cycle present in larger C-C bond lengths than the corresponding equilibrium value, and these correlate with the distance from the center of the sample (i.e., with the initial stress of the compressed sample). It is noticeable that the tensile stress generated in the recovered samples correlates with the compressive stress applied; for instance, at 35 μm from the center of the sample, the *G* band downshifts about 12 cm^{-1} , while at 60 μm from the center, the downshift is only close to 5 cm^{-1} , which correspond to tensile strains of about 0.14 and 0.05%, respectively.

Interestingly, an analogous effect is observed for the double-resonant intervalley *D* band; this is not surprising based on the atomic motions that originate this band, which are depicted in Fig. 2(c). However, these results must be carefully analyzed because there are important quantitative differences compared with the above analysis of the *G* band. The larger shifts observed in compression for the *D* band are a consequence of its larger average Grüneisen parameter in the compression regime.¹¹ For instance, the frequency of the *D* band in the spectrum measured at 35 μm from the center of the compressed sample is 25 cm^{-1} above the reference value at room conditions (1352 cm^{-1} at 532 nm excitation). What is surprising is the behavior of the *D* band observed in the recovered samples, since the downshift of the *D* band (2 cm^{-1} at 35 μm from the center of the recovered sample) is much smaller than that of the *G* band (12 cm^{-1}). Analogous differences were obtained along three sampling radial paths. This indicates that the *G* band is more sensitive to tensile strains than the *D* band, and the opposite happens under compressive strain.

Another remarkable result concerns the changes in the relative intensity of the *D* band because of its relation with defects.^{25,26} All of the defect-mediated bands (*D*, *D'*, and *D + D'*) can be barely observed in pristine graphitic samples,²⁷ but all of these bands increase their intensities upon compression. Such intensity enhancement under compressive stress is still unclear; the natural explanation is an increase in the defect concentration induced by the strain, but the strain dependence of the Raman cross sections of these bands is still poorly understood,¹⁸ and further studies are required to clarify this effect. It seems reasonable that the residual stress accumulated upon compression derives into the creation of defects after decompression, as revealed by the large intensity enhancement observed for all of the defect-related bands in the recovered samples. In this regard, an analysis of the intensity changes observed for the double-resonant intravalley *D'* band, which appears as a shoulder of the *G* band at 1623 cm^{-1} at room conditions and 532 nm excitation, is required. Our results confirm that the (*D/D'*) intensity ratio in the uncompressed samples remains constant in about 14, regardless of the value of the residual tensile strain present in different areas of

the sample, which is in excellent agreement with previous results.²⁶ However, we noticed that this ratio varies under strain and again confirms that a further study on the strain dependence of the Raman cross sections in graphitic materials is demanding. In any case, according to recent theoretical results,²⁸ it appears that only hopping defects are generated in our experiments; this is an observation compatible with the idea that along a biaxial compression-decompression cycle, deformation of the C-C bonds takes place without changing the hybridization of the graphene sheets.

We have also calculated the Grüneisen parameter of the *D* band, γ^D , as a function of the strain, using the following relation: $\gamma^D = \gamma^G \frac{\omega_G}{\omega_D} \frac{d\omega_D}{d\omega_G}$, where ω_i represents the Raman shift of each band at a given strain. We have used a constant average value of 1.8 for the Grüneisen parameter of the *G* band, γ^G ,^{23,29,30} this is possible because recent calculations confirm that this parameter exhibits negligible variation over the strain range considered here.³¹

The results plotted in Fig. 3(a) confirm that γ^D is strongly strain dependent, showing opposite behavior in the compressive (increasing γ^D) and tensile (decreasing γ^D) regimes. This conclusion contrasts with the data compiled by Ferralis³² for both graphene and graphite under different strain conditions. However, it must be noticed that most Grüneisen parameters available were calculated from strain (or pressure) slopes and the corresponding elastic compliances.^{13,32} Furthermore, most γ^D have been, in fact, obtained from γ^{2D} values.³² To our knowledge, only Ding *et al.*¹¹ have reported a real value of γ^D in graphene and their results agree with our observations. In order to check whether our results are intrinsically consistent, we compare twice the frequency ω_D with our measured frequencies for the two contributions of the 2*D* band [2*D*1 and 2*D*2 in Fig. 2(d)]. Again, a nonlinear behavior is found for the two 2*D* contributions; a quite different strain slope is observed under compressive or tensile conditions. An almost constant variation is found for tensile strain, which is in agreement with previous studies of bulk graphite samples subjected to uniaxial tension.¹⁶ Despite the apparent coincidence between

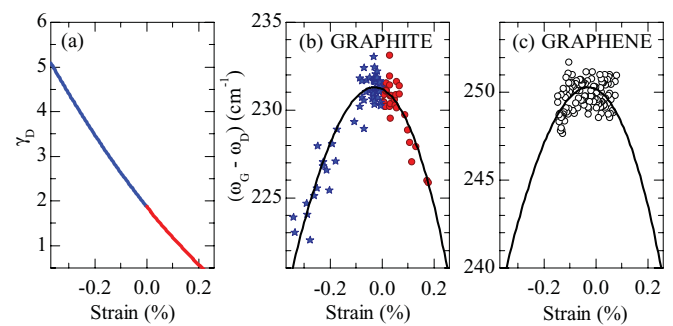


FIG. 3. (Color online) (a) Calculated Grüneisen parameter of the *D* band. (b), (c) Frequency difference between the *G* and *D* bands as a function of the strain. The blue/dark gray stars correspond to the compressed sample and the red/gray circles correspond to the expanded one. The open circles are the biaxial strain results, reproduced from Ref. 11, measured in graphene. In (b), the line represents a cubic fitting function to our results. In (c), this function has been shifted 19 cm^{-1} to match the frequency difference between the *G* and *D* bands in monolayer graphene at zero strain.

BRIEF REPORTS

PHYSICAL REVIEW B 00, 003400 (2012)

the $2\omega_D$ and ω_{2D1} (the characteristic feature in graphene) frequencies, the observed differences confirm that they are different contributions.¹¹ Thus, all of our observations again suggest that the use of published γ^{2D} values to estimate the strain in graphene and graphite-related materials must be revisited, as recently pointed out in experimental and theoretical studies.³³

In any case, the dramatic nonlinear behavior observed for ω_D as a function of the strain leads to the conclusion that it can be used as a practical local-strain scale. To check this possibility, we plot in Fig. 3(b) the difference $(\omega_G - \omega_D)$ under both compressive and tensile regimes, and we observe that this difference always decreases with respect to the value measured under ambient conditions (232 cm^{-1} for graphite and 249 cm^{-1} for graphene at 532.0 nm excitation). At small strains (0.2%), we already detect notable changes in the measured Raman frequencies, so the quantity $(\omega_G - \omega_D)$ is revealed as an interesting strain gauge. In order to confirm our results, we compare our results to those recently reported in graphene under both compressive and tensile biaxial strains.¹¹ In Fig. 3(c), we compare our prediction for graphene with results adapted from Ding *et al.*¹¹ Our results have been shifted to match the value measured in graphene at room conditions. Our prediction matches the results obtained in graphene, although the nonlinear dependence was not observed by these authors because strains as low as 0.1% were reported. Interestingly, a closer look at Fig. 2 in Ref. 11 reveals an incipient nonlinear dependence of the $2D$ band in the vicinity of 0.1% strain in both compressive and tensile regimes.

In summary, as the most prominent bands in the Raman spectrum of carbon materials are associated to phonons of different points of the first Brillouin zone of graphite and graphene, i.e., the G band is related to a phonon in the Γ point whereas the D and $2D$ bands are due to phonons around

the \mathbf{K} point,⁸ the results presented in this Brief Report reveal that biaxial strain has quite different effects on the electronic structure around \mathbf{K} and Γ points, as revealed by the different strain dependencies of the G band and the double-resonance D and $2D$ bands. The strong nonlinear dependencies with the biaxial strain observed for the D and $2D$ bands convey drastic variations in their corresponding Grüneisen parameters, therefore caution is recommended when using the current proposals to evaluate the strain using Raman spectroscopy. Our results also suggest an interesting application of Raman spectroscopy because the frequency difference $(\omega_G - \omega_D)$ gives a direct measure of the strain in graphite and related materials. In undefective samples, were the D band cannot be observed, the relevant quantity should be $(\omega_G - \omega_{2D})/2$. This correlation should be particularly useful in the case of graphene samples, since both G and $2D$ bands are the most prominent features in the Raman spectrum and both exhibit highly symmetric band shapes. Finally, let us emphasize that earlier studies using anvil devices were unsuitable to observe the phenomena described in this Brief Report because of the interference of the overwhelming signal of the diamond anvil, which is centered around 1332 cm^{-1} . This again confirms the advantage of using moissanite or sapphire anvils to study graphite-related samples under large compressions, provided that the background contribution of the anvil is properly subtracted.²²

This research was supported by the Ministerio de Ciencia e Innovación under Project No. CTQ2009-14596-C02-01 and MALTA-Consolider Ingenio 2010 (Project No. CSD2007-00045). Funding was also provided by Comunidad de Madrid under Program No. QUIMAPRES-S2009/PPQ-1551 and Grant No. UCM-BSCH-910481 from the Universidad Complutense de Madrid. E.d.C. is grateful to the Spanish Ministerio de Educación for an FPU grant.

*edelcorro@quim.ucm.es

¹J. P. Lu, *Phys. Rev. Lett.* **79**, 1297 (1997).

²M. F. Yu, O. Lourie, M. J. Dyer, K. Moloni, T. F. Kelly, and R. S. Ruoff, *Science* **287**, 637 (2000).

³C. Lee, X. D. Wei, J. W. Kysar, and J. Hone, *Science* **321**, 385 (2008).

⁴E. Cadelano, P. L. Palla, S. Giordano, and L. Colombo, *Phys. Rev. Lett.* **102**, 235502 (2009).

⁵C. Thomsen and S. Reich, *Phys. Rev. Lett.* **85**, 5214 (2000).

⁶R. Saito, A. Jorio, A. G. Souza Filho, G. Dresselhaus, M. S. Dresselhaus, and M. A. Pimenta, *Phys. Rev. Lett.* **88**, 027401 (2001).

⁷J. Maultzsch, S. Reich, and C. Thomsen, *Phys. Rev. B* **70**, 155403 (2004).

⁸A. C. Ferrari, *Solid State Commun.* **143**, 47 (2007).

⁹O. Frank, G. Tsoukleri, I. Riaz, K. Papagelis, J. Parthenios, A. C. Ferrari, A. K. Geim, K. S. Novoselov, and C. Galiotis, *Nature Commun.* **2**, 255 (2011).

¹⁰T. M. G. Mohiuddin, A. Lombardo, R. R. Nair, A. Bonetti, G. Savini, R. Jalil, N. Bonini, D. M. Basko, C. Galiotis, N. Marzari, K. S. Novoselov, A. K. Geim, and A. C. Ferrari, *Phys. Rev. B* **79**, 205433 (2009).

¹¹F. Ding, H. Ji, Y. Chen, A. Herklotz, K. Dörr, Y. Mei, A. Rastelli, and O. G. Schmidt, *Nano Lett.* **10**, 3453 (2010).

¹²J. E. Proctor, E. Gregoryanz, K. S. Novoselov, M. Lotya, J. N. Coleman, and M. P. Halsall, *Phys. Rev. B* **80**, 073408 (2009).

¹³J. Nicolle, D. Machon, P. Poncharal, O. Pierre-Louis, and A. San-Miguel, *Nano Lett.* **11**, 3564 (2011).

¹⁴M. Huang, H. Yan, C. Chen, D. Song, T. F. Heinz, and J. Hone, *Proc. Natl. Acad. Sci. USA* **106**, 7304 (2009).

¹⁵Z. H. Ni, T. Yu, Y. H. Lu, Y. Y. Wang, Y. P. Feng, and Z. X. Shen, *ACS Nano* **2**, 2301 (2008).

¹⁶G. Tsoukleri, J. Parthenios, K. Papagelis, R. Jalil, A. C. Ferrari, A. K. Geim, K. S. Novoselov, and C. Galiotis, *Small* **5**, 2397 (2009).

¹⁷O. Frank, G. Tsoukleri, J. Parthenios, K. Papagelis, I. Riaz, R. Jalil, K. S. Novoselov, and C. Galiotis, *ACS Nano* **4**, 3131 (2010).

¹⁸M. Mohr, J. Maultzsch, and C. Thomsen, *Phys. Rev. B* **82**, 201409 (2010).

¹⁹J.-A. Xu and H.-K. Mao, *Science* **290**, 783 (2000).

²⁰V. G. Baonza, M. Taravillo, A. Arencibia, M. Cáceres, and J. Nuñez, *J. Raman Spectrosc.* **34**, 264. (2003).

²¹E. Del Corro, J. González, M. Taravillo, E. Flahaut, and V. G. Baonza, *Nano Lett.* **8**, 2215 (2008).

BRIEF REPORTS

PHYSICAL REVIEW B **00**, 003400 (2012)

²²E. Del Corro, M. Taravillo, J. González, and V. G. Baonza, *Carbon* **49**, 973 (2011).

²³M. Hanfland, H. Beister, and K. Syassen, *Phys. Rev. B* **39**, 12598 (1989).

²⁴A. F. Goncharov, *High Press. Res.* **8**, 607 (1992).

²⁵A. C. Ferrari and J. Robertson, *Phys. Rev. B* **61**, 14095 (2000).

²⁶L. G. Cançado, A. Jorio, and M. A. Pimenta, *Phys. Rev. B* **76**, 064304 (2007).

²⁷Y. Kawashima and G. Katagiri, *Phys. Rev. B* **52**, 10053 (1995).

²⁸P. Venezuela, M. Lazzeri, and F. Mauri, *Phys. Rev. B* **84**, 035433 (2011).

²⁹L. Zhenxian, W. Lizhong, Z. Yongnian, C. Qilang, and J. Guangtian, *J. Phys. Condens. Matter* **2**, 8083 (1990).

³⁰J. Sandler, M. S. P. Shaffer, A. H. Windle, M. P. Halsall, M. A. Montes-Moran, C. A. Cooper, and R. J. Young, *Phys. Rev. B* **67**, 035417 (2003).

³¹Y. C. Cheng, Z. Y. Zhu, G. S. Huang, and U. Schwingenschlögl, *Phys. Rev. B* **83**, 115449 (2011).

³²N. Ferralis, *J. Mater. Sci.* **45**, 5135 (2010).

³³O. Frank, M. Mohr, J. Maultzsch, C. Thomsen, I. Riaz, R. Jalil, K. S. Novoselov, G. Tsoukleri, J. Parthenios, K. Papagelis, L. Kavan, and C. Galiotis, *ACS Nano* **5**, 2231 (2011).